Theor Appl Climatol (2010) 100:23–27
DOI 10.1007/s00704-009-0159-0

ORIGINAL PAPER

On the 60-month cycle of multivariate ENSO index

Adriano Mazzarella · Andrea Giuliacci · Ioannis Liritzis

Received: 12 January 2009 / Accepted: 8 June 2009 / Published online: 8 July 2009

Abstract Many point indices have been developed to describe El Niño/Southern Oscillation, but the multivariate El Niño Southern Oscillation (ENSO) index (MEI) is considered the most representative since it links six different meteorological parameters measured over the tropical Pacific. Spectral analysis with appropriate data reduction techniques of monthly values of MEI (1950–2008) has allowed the identification of a large 60-month cycle, statistically confident at a level larger than 99%. The highest values of MEI (typical of El Niño events) and the lowest values of MEI (typical of La Niña events) are concordant with respective maxima and minima values of the identified 60-month cycle.

1 Introduction

The monitoring of the El Niño/Southern Oscillation (ENSO) phenomenon is normally based on observations of sea surface temperatures (averaged to single values over large regions within the equatorial Pacific Ocean identified as Niño 4, Niño 3, and even Niño 3.4) and on the difference between Tahiti and Darwin atmospheric pressure in the whole tropical Pacific Basin (Rasmusson and Carpenter 1982; Ropelewski and Jones 1987; Allan et al. 1991; Trenberth 1997; Können et al. 1998). Such point measures are useful indicators of the ENSO phenomenon, but not representative of the coupled ocean–atmosphere phenomenon: the complexity of the climate system cannot be understood on the basis of simple and point measures. A more holistic approach has been developed at NOAA's Climate Diagnostics Center in Boulder Colorado with multivariate ENSO index (MEI) that is derived from tropical Pacific Comprehensive Ocean–Atmosphere Data Set (COADS) (Wolter and Timlin 1993, 1998). MEI is a multivariate measure of the ENSO signal in the first principal component of six main observed variables over the tropical Pacific: sea level pressure, zonal and meridional components of the surface wind, sea surface temperature, surface air temperature, and cloudiness of the sky. The highest values of MEI values represent the warm ENSO phase (El Niño) while the lowest values of MEI represent the cold ENSO phase (La Niña). MEI index time series has not been yet visited on a statistical elaboration, and here, we perform a robust statistical analysis while investigating the underlying physical processes.

2 Data set and analysis

The data consist of the monthly values of MEI (period 1950–2008) as computed by Wolter and Timlin (1993, 1998), taken from the web site http://www.cdc.noaa.gov/people/klaus.wolter/MEI/table.html, where each monthly value is centered between the preceding and subsequent month: for example, the January value represents the value

A. Mazzarella (✉) · A. Giuliacci
Meteorological Observatory, Department of Earth Science,
University of Naples Federico II,
Largo S. Marcellino,
10 80138 Naples, Italy
e-mail: adriano.mazzarella@unina.it

A. Giuliacci
e-mail: andrea.giuliacci@yahoo.it

I. Liritzis
Laboratory of Archaeometry,
Department of Mediterranean Studies, University of the Aegean,
Mytilene 85100, Greece
e-mail: liritzis@rhodes.aegean.gr

centered between the December–January and so on. The MEI is a weighted average of the ENSO-associated features contained in the combined six variables. In the COADS data set, these variables are available at a sufficient resolution such that large-scale patterns (as opposed to point measurements) can be used in relation to each other to get a more comprehensive measure of ENSO-related interactions. The MEI values are standardized with respect to a 1950–1993 reference period and are computed as the first unrotated principal component (PC) (Miranda et al. 2008) of all six combined observed fields. This is accomplished by normalizing the total variance of each field first and then performing the extraction of the first PC on the covariance matrix of the combined field. The series of MEI monthly values are expressed as percentages of standard deviation for which it has a total mean equal to 0 and a standard deviation equal to 1 (Fig. 1). Spectral and autocorrelation analyses were applied to the available MEI monthly values and the results were obtained according to 47 degrees of freedom. At first sight, it appears that the autocorrelation coefficients (Fig. 2a) exhibit a decreasing and oscillating behavior while the normalized power spectrum (Fig. 2b), obtained as Fourier transform of autocorrelation coefficient, shows a concentration of energy between 60 and 20 months that explains almost all the monthly MEI variance. To obtain a more detailed information on the main harmonics constituting MEI monthly series, two separate and specific statistical methods are here employed: the vector probable (vpe) and the phase averaging analysis. Both methods subdivide the entire observation interval into non-overlapping subintervals (with a length equal to the period of the harmonic to be investigated) after the filtering of non-cyclic variation performed according to the least-square analysis.

A: The first approach consists in the calculation of the Fourier coefficients for each of the subintervals and of the scattering of the individual harmonics from the center of gravity A of all points, corresponding to the harmonic coefficients as computed from all series. The reliability is computed according to the vector probable error (vpe) equal to the root-mean-square radius of the point cloud. The confidence level of the harmonic is computed according to the equation: $1 - \exp[-(0.833\ A/\text{vpe})^2]$. The harmonic is found to be confident at 95% (99%) level when $A \geq 2.08$ vpe ($A \geq 3.00$ vpe) (Cecere et al. 1981).

B: The second approach regards the calculation of the correlation coefficient R among the N monthly values, constituting the mean investigated cycle, and those computed according to the first Fourier harmonic. To evaluate the accuracy of R, we have computed the random variable $W = 0.5 \ln[(1|R)/(1-R)]$ that has an approximately normal distribution with a mean equal to $0.5 \ln[(1|R)/(1-R)]$ and a variance equal to $(N-3)^{-1}$ (Bendat and Piersol 1971; Mazzarella and Palumbo 1994). The level of confidence of R is obtained by testing W (normalized to a mean equal to 0 and to a variance equal to 1) versus the null hypothesis of zero population relationship according to the standard one-sided z test. The harmonic is found to be confident at 95% (99%) level when the relationship $W = \sqrt{(N-3)/2}\ \ln(1+R)/(1-R)$ provides values ≥1.96 (≥2.58).

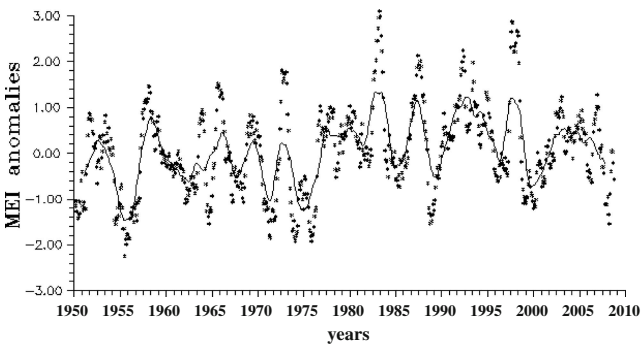

Fig. 1 Time series plot of MEI monthly values from January 1950 to December 2008 (*star points*); the *continuous line* represents the 25-month running mean

3 Results

After several trials, we have found that the values of vpe and R are the highest and confident at a level larger than 99% only when we subdivide the MEI series into subintervals of 26 and 60 months. The Fourier synthesis of 26- and 60-month harmonics is found to account for more than 25% of the total monthly MEI variability. To further reinforce the evidence of both harmonics, we smoothed the available monthly MEI series according to different running means; such a smoothing is equivalent to a low-pass filtering which allows the removal of all the oscillations with periods shorter than the chosen cut-period with a small reduction in amplitude but no phase shift (Bendat and Piersol 1971; Mazzarella and Palumbo 1994).

Figure 3 reports the plot of the average 26-month cycle of MEI, smoothed according to a 5-month running mean to eliminate all the oscillations shorter than 5 months. The 26-month periodic variation appears with a high statistical stability even if with a low energetic level. Figure 4 shows the plot of the average 60-month cycle of MEI, smoothed according to a 25-month running mean, to eliminate all the oscillations shorter than 25 months (because of the utilized smoothing process, the smoothed series is operative from 1951 to 2007): The 60-month march appears with a high statistical stability and a high power. The values of

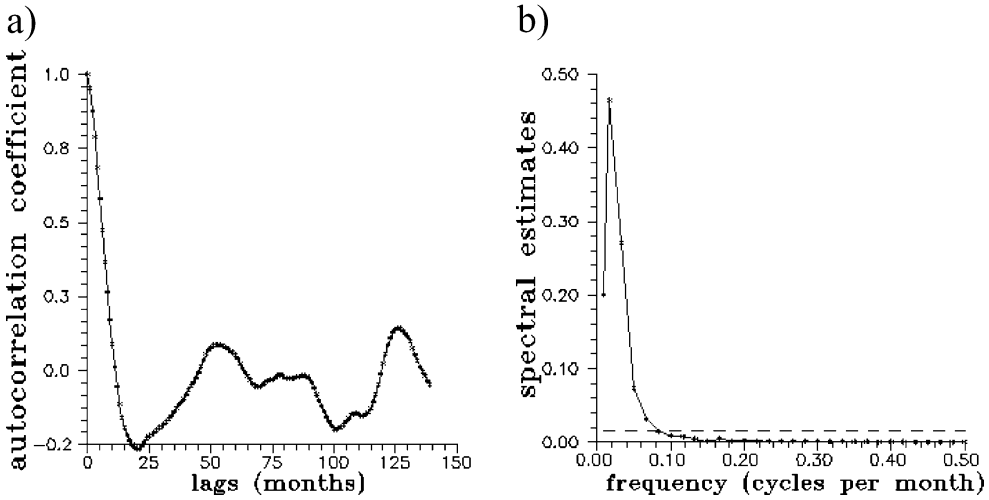

Fig. 2 **a** Autocorrelation coefficient of monthly MEI series for various time lags. **b** Normalized spectral estimates of monthly MEI series. The *dashed line* indicates the 95% confidence level of the equivalent white noise process based on 47 degrees of freedom

amplitude, phase, vpe, R, and confidence level of this harmonic are reported on Table 1. Figure 1 shows the plot of the monthly MEI values, smoothed according to a 25-month running mean.

4 Discussion

The El Niño Southern Oscillation is the Earth's strongest natural climate fluctuation on inter-annual timescales and has quasi-global impacts although originating in the tropical Pacific; ENSO is a complex atmospheric and oceanographic phenomenon that has given rise to profound economic and social consequences (Wang and Fiedler 2006 and references therein). The ENSO is well described by MEI index that combines six representative meteorological indices measured in the tropical Pacific. The use of MEI provides a more holistic description of the ENSO phenomenon than other point indices do; really, the sea surface temperature or the simple difference of atmospheric pressure between Darwin and Tahiti provide a much more reductionist description. The application of two different statistical analyses to the available monthly MEI has evidenced two harmonics of 26- and 60-month periods, confident at a level greater than 99% (Figs. 3 and 4), whose Fourier synthesis accounts for more than 25% of the overall monthly MEI variability. The 26-month cycle would suggest a possible relationship between the series of MEI and that of the tropical stratospheric winds that follow the quasi-biennial oscillation with a dominant period equal to 28 months (Baldwin et al. 2001), which is different from that here identified. The presence of a clear and statistically confident 5-year cycle in the MEI has been here ascertained for the first time. Fedorov et al. (2003) identified the same 5-year pattern in the ENSO time occurrence, but such a harmonic is so damped and sustained by random distur-

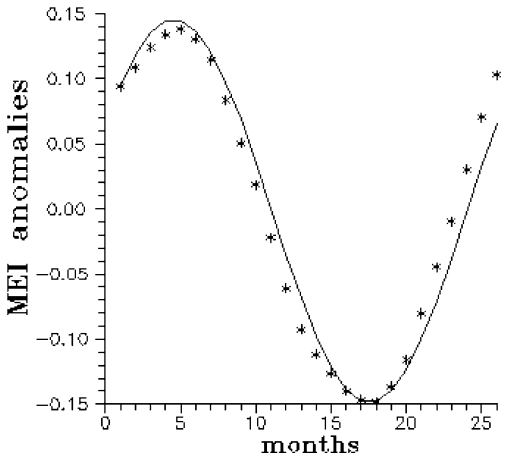

Fig. 3 Average 26-month cycle of the 5-month running mean of MEI. The *continuous curve* represents the first Fourier harmonic

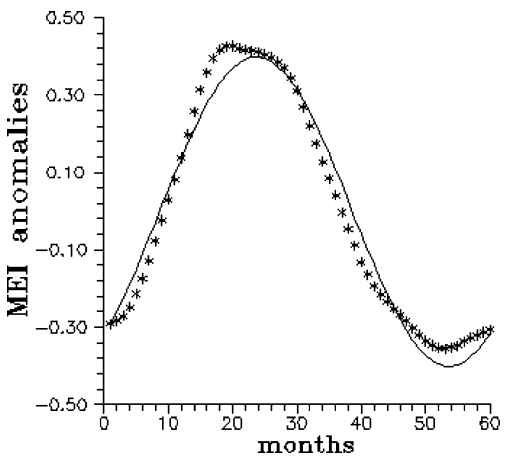

Fig. 4 Average 60-month cycle of the 25-month running mean of MEI. The *continuous curve* represents the first Fourier harmonic

Table 1 Values of amplitude (A), phase (ϕ), vpe, and confidence level of the 26- and 60-month cycles obtained from the monthly values of MEI, available from 1950 to 2008, and smoothed according to a 5- and a 25-month running mean, respectively

Period (months)	N	A	ϕ	vpe	A/vpe	R	Confidence level
26	26	0.21	−14.3°	0.11	1.91	0.95	Larger than 92%
60	11	0.40	−45.8°	0.12	3.34	0.99	Larger than 99%

N and R represent the number of subintervals and the correlation coefficient among the 60 monthly observed MEI values and computed according to the first Fourier harmonic

bances to allow El Niño prediction only at probabilistic scale; equally, Hiromitsu (2004) evidenced a 5-year period in the north–south pressure difference series in Japan, largely influenced by El Niño occurrence and commonly utilized to forecast summer weather. If the 60-month harmonic is to be usefully utilized as a predictor of El Niño and La Niña occurrences, we can verify its forecasting power in the past. To perform such a test, a comparison is made, for each month "t", between the values of the 25-month running mean of MEI (that shows a mean equal to 0) and the MEI synthetic values derived from the equation: $\mathrm{MEI}(t) = A \sin[(360/60)/t - \phi)]$, where A=0.40 and ϕ=−45.8° (Table 1). Figure 5 reports the simultaneous plot of both the series; positive values greater than 0.7 represent warm events (El Niño) and negative events (less than −0.7) cool events (La Niña). It appears that all El Niño events occurred in the past (like in 1958.2, equal to 0.79, in 1982.8, equal to 1.33, in 1987.4, equal to 1.14, in 1992.8, equal to 1.23, and in 1997.7, equal to 1.20) are found to occur in correspondence of maxima values of the 60-month cycle; equally, all La Niña events occurred in the past (like in 1955.6, equal to −1.47, in 1975.0, equal to −1.25, and in 1999.8, equal to −0.74) are found to occur in correspondence of minima values of the 60-month cycle. In spite of the small amplitude of the 60-month cycle, the maxima and minima of 60-month harmonic can be reasonably considered to be a necessary (though not sufficient) conditions of the El Niño and la Niña occurrence. The two series appear to be out of phase only during the 1962–1970 interval. If we were to force the forecasting after 2008, the 60-month cycle suggests a possible estimate for the possible coming El Niño occurrence around the year 2013 and for La Niña occurrence around the year 2016.

5 Conclusion

The MEI index is found to be more representative of El Niño Southern Oscillation in respect to the numerous available point indices. It appears that the maxima and minima of MEI 60-month cycle can be reasonably considered as an existing periodic forcing and a necessary (even if not sufficient) condition of the El Niño and La

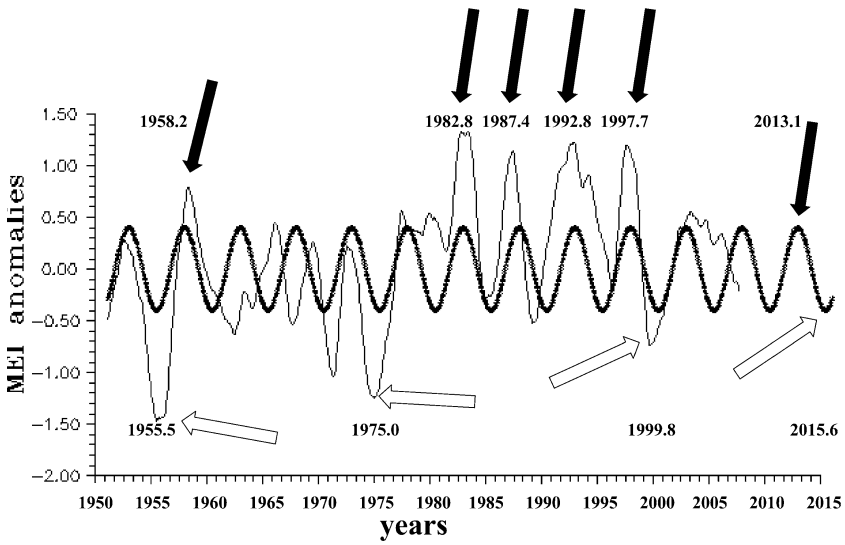

Fig. 5 Time series plot of the 25-month running mean of MEI from January 1951 to December 2007; the *solid line* represents the 60-month cycle extrapolated to 2015. The *black arrows* are relative to El Niño time occurrences while the *white arrows* are relative to La Niña time occurrences

Niña occurrence; such a cycle suggests an estimate for the coming El Niño occurrence around the year 2013 and for the coming La Niña occurrence around the year 2016.

References

Allan RJ, Nicholls N, Jones PD, Butterworth IJ (1991) A further extension of the Tahiti Darwin SOI, early SOI results and Darwin pressure. J Climate 4:743–749

Baldwin MP, Gray LJ, Dunkerton TJ, Hamilton K, Haynes PH, Randel WJ, Holton JR, Alexander MJ, Hirota I, Horinouchi T, Jones DBA, Kinnersley JS, Marquardt C, Sato K, Takanashi M (2001) The quasi biennal oscillation. Rev Geophys 39:179–229

Bendat JS, Piersol AG (1971) Random data analysis: measurement procedures. Wiley-Interscience, New York p 407

Cecere A, Mazzarella A, Palumbo A (1981) TIDE: a computer program of refinement of the Chapman–Miller method for the determination of lunar tides. Comput Geosci 7:185–198

Fedorov AV, Harper SL, Philander G, Winter B, Wittenberg A (2003) How predictability is El Niño? Bull Am Meteorol Soc 84:911–919

Hiromitsu K (2004) Five-year cycle of north–south pressure difference as an index of summer weather in northern Japan from 1982 onwards. J Meteorol Soc Jpn 82:711–724

Können GP, Jones PD, Kaltofen MH, Allan RJ (1998) Pre-1866 extensions of the Southern Oscillation index using early Indonesian and Tahitian meteorological readings. J Climate 11:2325–2339

Mazzarella A, Palumbo A (1994) The lunar nodal induced-signal in climatic and oceanic data over the Western Mediterranean area and on its bistable phasing. Theor Appl Climatol 50:93–102

Miranda AA, Le Borgne YA, Bontempi G (2008) New routes from minimal approximation error to principal components. Neural Proc Lett 27:197–207

Rasmusson EG, Carpenter TH (1982) Variations in tropical sea surface temperature and surface wind fields associated with the Southern Oscillation/El Niño. Mon Weather Rev 110:354–384

Ropelewski CF, Jones PD (1987) An extension of the Tahiti–Darwin Southern Oscillation index. Mon Weather Rev 115:2161–2165

Trenberth KE (1997) The definition of El Niño. Bull Am Meteorol Soc 78:2771–2777

Wang C, Fiedler PC (2006) ENSO variability and the eastern tropical Pacific: a review. Prog Oceanogr 69:239–266

Wolter K, Timlin MS (1993) Monitoring ENSO in COADS with a seasonally adjusted principal component index. Proceedings of the 17th Climate Diagnostics Workshop, Norman, OK, NOAA/N MC/CAC, NSSL, Oklahoma Climate Survey, CIMMS and the School of Meteorology, University of Oklahoma, pp 52–57

Wolter K, Timlin MS (1998) Measuring the strength of ENSO events—how does 1997/98 rank? Weather 53:315–324